Int. J. Heat Mass Transfer. Vol. 31, No. 4, pp. 895–898, 1988
Printed in Great Britain

0017–9310/88 $3.00+0.00

Penetrative double diffusive convection: effects of the Lewis and Prandtl numbers

BASIL N. ANTAR
Engineering Science and Mechanics, University of Tennessee Space Institute, Tullahoma, TN 37388, U.S.A.

(*Received* 28 *April* 1987 *and in final form* 16 *October* 1987)

1. INTRODUCTION

IN MANY naturally occurring phenomena, thermal convection happens in an unstably stratified fluid layer which is bounded from above and/or below by stably stratified regions. For such configurations the convective motion may extend a substantial distance into the adjacent stable zones. If the convective mixing is efficient enough, the stable thermal stratification may be weakened sufficiently to allow the motion to penetrate far deeper into the stable zones than might be predicted by studying the initial state. Such states of penetrative convection are the subject of the present study.

In an earlier paper [1], the onset of penetrative convection in a binary mixture fluid layer was studied. In that paper a coupled convection mechanism was investigated which was due to the presence of two diffusing components, widely separated in values and also possessing a density maximum in the interior of the fluid. To understand the physical processes involved in such motions, the model in ref. [1] was chosen to be as simple as possible, namely, an infinite fluid layer in which temperature and concentration varied linearly with height. The variation of density with temperature was assumed to be quadratic while it was assumed to be only linear with concentration. Attention was confined to the linear stability of that configuration and the study was further restricted to the case in which the temperature stratification was destabilizing while the concentration stratification was stabilizing. Nevertheless, this model was still somewhat complex and the analysis in ref. [1] was confined to Prandtl and Lewis numbers of 10 and 0.01, respectively. These parameter values realistically model a mixture of salt and water, and were chosen to allow for comparison with previous work on penetrative convection as well as on double diffusive convection with monotone density variation.

The present study should be viewed as an extension of the work performed in ref. [1] and was undertaken to cover the onset of convection for a wider range of both Prandtl and Lewis numbers. This is to allow for the application of penetrative double diffusive convection to a variety of fluid mixtures.

2. THE MODEL AND ITS SOLUTION

The model analyzed in this work is the same as that of ref. [1] and consists of a heated fluid layer of depth, d, which is infinite in the horizontal direction. The coordinate system is rectangular Cartesian with the x- and y-axes in the horizontal direction and z in the vertical. The fluid layer is assumed to support both constant temperature and constant concentration gradients in the vertical direction which are given by

$$\bar{T} = T_0 - (d_0 - z)\Delta T/d_0 \quad (1)$$

$$\bar{S} = S_0 + (d_0 - z)\Delta S/d \quad (2)$$

where T_0 and S_0 are the temperature and the solute concentration values at the specific vertical location, d_0. Equations (1) and (2) define the motionless basic state the stability of which is being analyzed.

Before proceeding with the convection analysis it is instructive to specify the response of the fluid density to small variations in both temperature and concentration. Customary analytical approaches to double diffusive convection, e.g. Turner [2], restrict the density variation of the fluid to be linear with both temperature and concentration changes. This is our point of departure from previous studies of double diffusive convection. This study will be concerned only with those fluids in which the density variation with temperature is quadratic. This is because the primary motivation for this study, as well as ref. [1], is to investigate the fluid response in a solidifying binary alloy that belongs to a certain class of mixtures characterized by this specific density variation within the fluid layer. A good representative of this class is the pseudo-binary system $Hg_{1-x}Cd_xTe$, which is normally assumed to be a mixture of mercury telluride, HgTe, and cadmium telluride, CdTe. The physical and chemical characteristics of this material have been under intensive scientific research due to its unique electronic and electro-optical properties [3]. Among the well-established physical properties for this system is the density variation of the liquid phase with both temperature and concentration. Figure 1 shows this variation as measured by Chandra and Holland [4] for three mole fractions, x. It is clearly seen in this figure that the measured densities possess maxima in the neighborhood of the freezing point for at least a moderate range of the mole fraction x for mercury rich mixtures. This variation of the density with temperature and concentration appears to be well approximated in the range of mole fraction, x, for $0 < x < 0.10$ by the following equation:

$$\rho = 7.931\{1 - 1.3515\times10^{-6}(T-1028)^2 - 3.1819\times10^{-3}(S-5)\} \quad (3)$$

where ρ is in g cm^{-2}, T in K, and S in percent mole fraction (i.e. $S = 100x$).

The intent of this study is to investigate the influence of such a density variation on the onset of double diffusive convection. Thus, in the following, the density dependence on temperature and concentration will be assumed to obey

$$\rho = \rho_0[1 - \alpha(T-T_0)^2 + \beta(S-S_0)] \quad (4)$$

where

$$\alpha = \frac{\partial\rho}{2\rho T\partial T}, \quad \beta = \frac{1\partial\rho}{\rho\partial S}$$

and ρ_0 is the density at temperature T_0 and concentration, S_0. In this case the height, d_0, is the position of maximum density when $\Delta S = 0$.

The linearized Boussinesq equations for the perturbation functions w, T and S with the density representation (4) and for the basic state (1) and (2) takes the following form:

$$\left[\frac{p}{\sigma} - (D^2 - a^2)\right](D^2 - a^2)w = a^2(1 - \lambda_0 z)T + a^2 S Rs \quad (5)$$

$$[p - (D^2 - a^2)]T = -Rw \quad (6)$$

$$[p - L(D^2 - a^2)]S = w \quad (7)$$

where $D = d/dz$. The boundary conditions on the perturbation functions for free upper and lower surfaces takes the form [1]

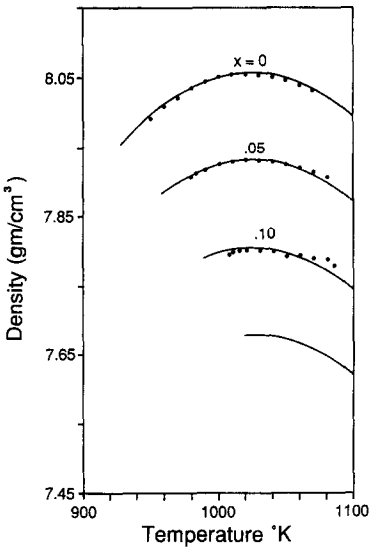

FIG. 1. Density variation of $Hg_{1-x}Cd_xTe$ with temperature and concentration: ●, measured data of ref. [4]; ——, equation (3).

$$w = D^2w = S = T = 0, \quad \text{at } z = 0, 1. \tag{8}$$

Here, R, Rs, L and σ are the Rayleigh, solutal Rayleigh, Lewis, and Prandtl numbers, respectively, and are defined as follows:

$$R = \frac{2\lambda_0^4 \alpha g (\Delta T)^2 d_0^3}{\kappa \nu}; \quad Rs = \frac{\beta g \Delta S d^3}{\kappa \nu};$$

$$L = \frac{\kappa_s}{\kappa}; \quad \sigma = \frac{\nu}{\kappa}; \quad \lambda_0 = \frac{d}{d_0}$$

where g, κ, κ_s, and ν are the gravity constant, the coefficients of thermal and mass diffusion and the kinematic viscosity, respectively. In equations (5)–(7) a is the horizontal wave number, which is real, while p, $p = p_r + ip_i$, is the complex frequency. p_r, is the perturbation growth rate, and p_i, the perturbation frequency. The complete derivation of the equations with the assumptions and justifications used may be found in ref. [1].

The homogeneous set of equations (5)–(7) with the homogeneous boundary conditions (8) form an eigenvalue problem that can be represented in the following functional form:

$$p = p(a, \lambda_0, R, Rs, \sigma, L). \tag{9}$$

This eigenvalue problem consists of a set of coupled linear, ordinary differential equations with six parameters. Such problems are solved by determining the eigenvalue, p (in this case both p_r and p_i), for specific values of the parameters involved in the equations. If, for a specific set of values of all the parameters in equation (9), p_r is found to be positive, then the perturbations are unstable, otherwise they are stable. A positive value for p_r, $p_r > 0$, implies that the motionless basic state will evolve into convective motion in the form of rolls or cells. Whenever several simultaneous eigenvalues exist for the same values of the parameters, the one with the largest value for p_r is called the mode of maximum growth rate. The monotone modes are those for which $p_i = 0$, for any p, while the oscillatory modes are those for which $p_i \neq 0$.

The results discussed in the next section were produced using the same technique as in ref. [1]. The details of the numerics and the various verifications of the computer codes used can be found there.

3. RESULTS AND DISCUSSION

In ref. [1] the results regarding the onset of convection were presented in the form of stability diagrams in the R–Rs plane, each for a different set of values of the parameters. Furthermore, the discussion in ref. [1] was limited to the first quadrant of the R–Rs plane because on the one hand, according to previous work [1, 2], both the monotone and the oscillatory modes of instability were found to possess maximum growth rates in this quadrant only. On the other hand, the original physical configuration envisioned and which motivated this study was one in which the temperature gradient of the basic state was destabilizing, $R > 0$, while the concentration gradient was stabilizing, $Rs > 0$. The results in ref. [1] indicated that the stability and instability regions in that section of the plane were delineated by two curves the positions of which depended on the parameter values used. Each set of two curves originated from a different position on the ordinate which are the points of critical instability belonging to the case of penetrative convection in a single component fluid. The two curves divided the first quadrant of the R–Rs plane into three distinct regions. The three regions were identified as regions I, II, and III and were defined in the following manner (see Fig. 2 of ref. [1]): in region I, all instability modes were damped and the basic state was stable to infinitesimal disturbances. In each of regions II and III there existed at least one unstable mode. The mode of maximum growth rate in region II was oscillatory ($p_r > 0$, $p_i \neq 0$), while in region III it was monotone ($p_r > 0$, $p_i = 0$). This specific division of the quadrant into the stable and unstable zones resemble the regime diagram for the classical double diffusive convection case discussed by Turner [2].

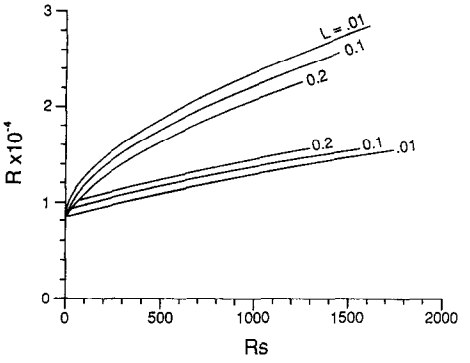

FIG. 2. Regions of stability and instability in the first quadrant of the R–Rs plane for $L = 0.01$, 0.1, and 0.2, and for $\lambda_0 = 2.0$ and $\sigma = 10$.

The analysis in ref. [1] also revealed that the division of the first quadrant of the R–Rs plane into the respective three regions was characteristic of the problem and changed only quantitatively with λ_0. As the value of λ_0 is increased, the position of the critical point of instability at $\Delta S = 0$ is shifted to higher Rayleigh numbers, R. Also, both of regions I and II appeared to increase substantially with increasing λ_0.

The intent here is to generalize the results of ref. [1] to a wider range of fluids possessing the specific density variation with temperature and concentration, as discussed in Section 2. To achieve this, the fundamental parameters entering the eigenvalue problem (9) and reflecting the different physical characteristics of the fluid are varied. These are the Prandtl and Lewis numbers, σ and L, respectively. Figure 2 illustrates the modification of the basic stability criteria brought about by changing the Lewis number. This figure shows the three stability and instability regions in the first quadrant of the R–Rs plane for three values of L and for fixed values of σ and λ_0 at 10.0 and 2.0, respectively. It is seen that as L is increased, the area of the plane where oscillatory modes of instability are dominant decreases while the stability zone grows. Also, for a fixed value of σ, the regions of dominant oscillatory unstable modes appear to be embedded within each other for successively higher values of L in such a way that the upper bound for this area is the one delineated for

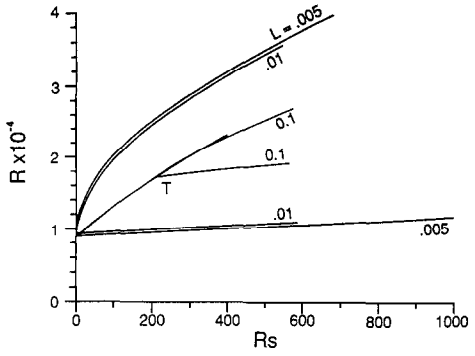

FIG. 3. Same as Fig. 2 but for $\sigma = 0.1$.

$L = 0.01$. Figure 2 suggests further that in the limit as $L \to \infty$, while σ is held constant, the width of the oscillatory unstable region, region II, will shrink in size to zero. Consequently it may be concluded that for this limiting case, only monotone modes possess maximum growth rates. Further analysis demonstrates that the three stability and instability zones which are delineated by the curves for $L = 0.01$ in Fig. 2 are very close to the asymptotic picture obtained in the limit as $L \to 0$. This implies that, as L approaches zero, the three characteristic stability and instability zones for this problem are not altered substantially from the respective zones shown for $L = 0.01$.

Figure 3 is similar to Fig. 2 except in this case a different Prandtl number is used. The variation of the three stability and instability zones with L are shown for $\lambda_0 = 2.0$ and $\sigma = 0.1$. Again, it is observed that the oscillatory unstable region diminishes in size with increasing L while the stable region grows. Also it is seen that the point at which the oscillatory region originates, labeled T in the figure, shifts to larger values for both R and Rs with increasing L. This point is also seen in Fig. 2 for both of the cases $L = 0.2$ and 0.1. For convenience the point will be called the triple point since it is the intersection of the three curves that divide the first quadrant of the R–Rs plane into the different stability and instability regions. It is observed that to the left of the triple point there exists only a single zone of instability which is separated from the stable region by the marginal stability curve. The stable region in this case is below the curve while the unstable region is above it. Furthermore, the unstable region to the left of the triple point is characterized by having only monotone modes of maximum growth rates. To the right of the triple point there exist the three customary regions of stability and instability. It should be pointed out that a triple point, at vanishingly small values of Rs, exists for each of the cases discussed here and in ref. [1]. However, some of these points evidently lie very close to the ordinate and are not visually discernible in the figures.

Figure 4 illustrates the modification of the stability and instability regime diagram, again in the same region of the R–Rs plane, as a result of variations in the value of the Prandtl number while L and λ_0 are held fixed. It shows a plot of the three regions for $\lambda_0 = 2.0$, $L = 0.1$, and $\sigma = 10.0$, 1.0, 0.1, and 0.05. Several interesting features are observed. First, it can be seen that the area in which the oscillatory modes are the most unstable shifts up diagonally with decreasing Prandtl numbers. This is manifested in the shift of the triple point to larger values of both R and Rs. The trend in this figure suggests that in the limit as $\sigma \to 0$, the triple point will have moved to very large values of both R and Rs leaving a substantial portion (if not all) of the first quadrant of the R–Rs plane devoid of a region in which the modes of maximum growth rates are oscillatory. Thus in the limit as $\sigma \to 0$, there will remain only one region of instability separated from the stable zone by the marginal stability curve. The modes of maximum growth rate in that unstable region are monotone. It is also observed that the zones of stability, region I, become larger with decreasing σ.

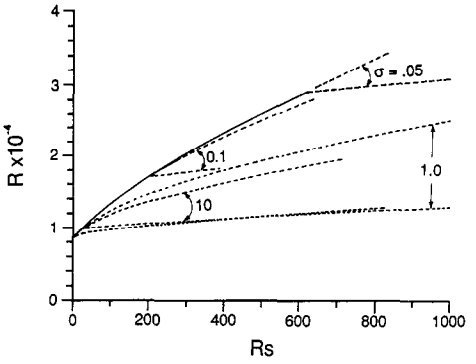

FIG. 4. Regions of stability and instability in the first quadrant of the R–Rs plane for $\sigma = 10$, 1, 0.1, and 0.05, and for $\lambda_0 = 2.0$ and $L = 0.1$.

The second feature observed in Fig. 4 is that all the regions where the most unstable modes are oscillatory appear to originate from a single smooth curve for different values of σ. This is the solid line in the figure. Further analysis shows that this curve can be constructed by establishing, in the R–Rs plane, the location of a second marginal stability mode, $p_r = 0$, in addition to the one delineating the lower boundary of region II, for the same values of σ, λ_0, L, and Rs. Depending on the value of σ, it is found that there exist two simultaneous modes in the first quadrant of the R–Rs plane possessing $p_r = 0$. One of these modes has $p_i = 0$ while the other has $p_i \neq 0$. The marginal stability modes making up the solid line in Fig. 4 are in fact neutral stability modes (i.e. $p_r = p_i = 0$). Whether two marginal stability modes exist for a single value of Rs, or only one, depends on the value of σ. Of course, whenever both modes exist, the one for which $p_i \neq 0$ occurs for a lower value of R and hence is the relevant one. This is the reason why the neutral stability curve shown in Fig. 4 was never discussed before. However, since the location of the neutral stability modes coincides with the locus of the triple points for all σ, the identification of their position in the R–Rs plane is very useful. As shown in Fig. 4, the curve on which these modes lie, forms an envelope for the oscillatory region, region II, in addition to the stable one, region I, for all values of σ. Thus this curve defines an absolute upper boundary for both the region of stable modes and the region of oscillatory most unstable modes in the first quadrant of the plane.

The qualitative modification of the three stability zones, as well as the presence of the envelope curve discussed above, were found to be independent of the specific value of λ_0. Figure 5 shows the various regions for $L = 0.1$, $\lambda_0 = 1.6$ and $\sigma = 1.0$, 0.1 and 0.05. This figure exhibits an almost identical trend to that shown in Fig. 4, except for the quantitative differences brought about by the values of the parameters. Note, however, that the curve delineating the upper boundary of region II and the locus of the triple points in Figs. 4 and 5 are not identical. There exists a small region in the R–Rs

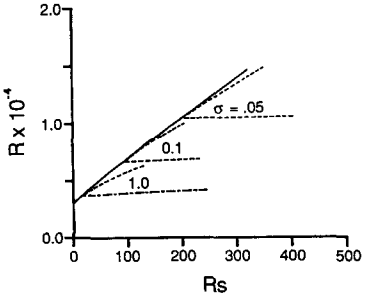

FIG. 5. Same as Fig. 4 but for $\lambda_0 = 1.6$.

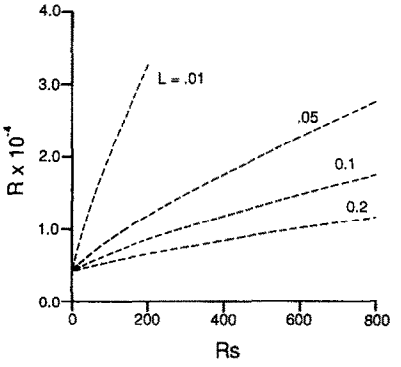

FIG. 6. The locus of the position of the triple points for $\lambda_0 = 2$, and for $L = 0.2, 0.1, 0.05$, and 0.01.

plane between these two curves in which the most unstable modes are oscillatory. The width of this region appears to diminish with decreasing σ and thus may not be discernible in these figures for lower values of σ, but nevertheless it exists.

The position of the solid curves in both Figs. 4 and 5 represents an absolute lower bound for the instability region in the first quadrant of the R–Rs plane. This is to say that any basic state configuration for which both R and Rs fall above that curve is linearly unstable. Thus the location of this curve is valuable as a general stability criteria for double diffusive convection.

Figure 6 shows the various envelope curves formed by the loci of the triple points for four Lewis numbers. Two significant features may be observed in this figure. The first is that all curves shown originate from a single point on the ordinate. This is the location of the critical point for $\Delta S = 0$. The second is that the inclination of each curve to the abscissa appears to increase with decreasing values of L. It may be concluded on the basis of this figure that the region in which the monotone unstable modes are dominant diminishes with decreasing L for any one value of Rs. However, this does not imply an equivalent increase in the stability region since, as was shown earlier, the size of that region is a function of σ. Depending on the value of σ there could be a substantial region below each of these curves in which the most unstable modes are oscillatory. It was also found that all curves shown in Fig. 6 collapse onto a single curve in the first quadrant of the R–Rs plane when plotted on an R–(Rs/L) scale (i.e. on a redefined Rs scale to $Rs' = \beta g \Delta S d^3/\kappa_s \nu$).

4. CONCLUSIONS

The analysis of the previous section revealed that the three stability and instability regions in the first quadrant of the R–Rs plane may be altered substantially by varying either σ or L. It was found that the region in which the oscillatory modes are found to possess maximum growth rates, in that portion of the plane, may diminish in size with increasing L. In fact, the results indicated that in the limit $L \to \infty$ only monotone modes possess maximum growth rates. This is a situation in which the instability is manifested by steady convective motion. This is also the case where mass diffusion has the dominant influence. Furthermore, it was found that for fluids possessing vanishingly small Prandtl numbers, again, only monotone modes have maximum growth rates for moderate values of both R and Rs. In this case, again, the instability is manifested by steady convection.

The analysis above lead also to the establishment of a simple general criterion for the onset of penetrative double diffusive convection. This was manifested by a single curve in the first quadrant of the R–Rs plane for all values of σ and L. The area above the curve comprises of a region of instability through monotone modes while below it the basic state configuration is either unstable through oscillatory modes or stable. There exists one such curve for every value of λ_0.

REFERENCES

1. B. N. Antar, Penetrative double diffusive convection, *Physics Fluids* **30**, 322–330 (1987).
2. J. S. Turner, *Buoyancy Effects in Fluids*, p. 251. Cambridge University Press, Cambridge (1973).
3. Proceedings of the 1983 U.S. Workshop on the physics and chemistry of mercury cadmium telluride, *J. Vac. Sci. Technol.* **A1**, 1579–1764 (1983).
4. D. Chandra and L. R. Holland, Density of liquid $Hg_{1-x}Cd_xTe$, *J. Vac. Sci. Technol.* **A1**, 1620 (1983).

Int. J. Heat Mass Transfer. Vol. 31, No. 4, pp. 898–902, 1988
Printed in Great Britain

0017–9310/88 $3.00 + 0.00

The relation between the rewetting temperature and the liquid–solid contact angle

S. OLEK† and Y. ZVIRIN
Department of Mechanical Engineering, Technion, Haifa 32000, Israel

and

E. ELIAS
Department of Nuclear Engineering, Technion, Haifa 32000, Israel

(*Received* 25 *July* 1986 *and in final form* 26 *October* 1987)

INTRODUCTION

DETERMINATION of the rewetting or minimum film boiling temperature is of great importance in reactor safety analysis during the reflooding phase of a hypothetical loss of coolant accident (LOCA). This temperature separates the high temperature region of a fuel pin where inefficient film boiling or vapor cooling takes place, from the lower temperature region, where more efficient transition boiling occurs. As the minimum film boiling temperature is the boundary between transition and film boiling its knowledge is required in the application of transition and film boiling correlations.

Two principal mechanisms are commonly proposed in the literature for the rewetting phenomenon.

†Present address: Swiss Federal Institute for Reactor Research (EIR), CH-5303 Würenlingen, Switzerland.